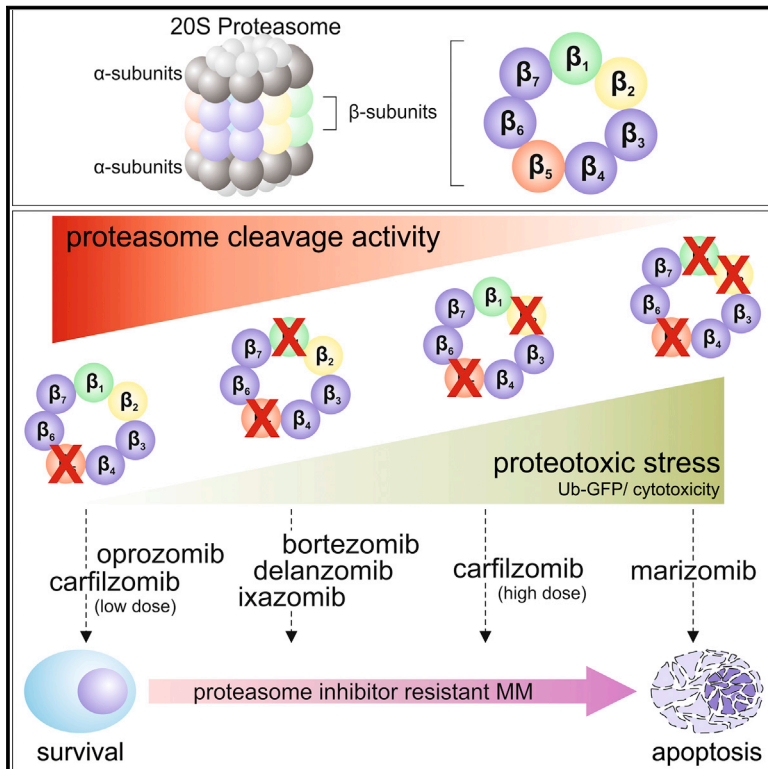


Cell Chemical Biology

Proteasome Inhibition in Multiple Myeloma: Head-to-Head Comparison of Currently Available Proteasome Inhibitors

Graphical Abstract



Authors

Andrej Besse, Lenka Besse, Marianne Kraus, ..., Elmer Maurits, Herman S. Overkleeft, Christoph Driessen

Correspondence

lenka.besse@kssg.ch or lenka.kubiczek@gmail.com

In Brief

Besse et al. demonstrate that clinically available proteasome inhibitors designed to target β_5 subunit are cytotoxic only when another proteasome subunit (β_1 or β_2) is co-inhibited. The co-inhibition of subunits is not equal and the most effective is $\beta_5 + \beta_2$ proteasome inhibition, effective also against proteasome inhibitor-resistant multiple myeloma.

Highlights

- Direct comparison of proteasome inhibitors by activity-based probes and Ub^{-G76V}-GFP
- Short-term β_5 inhibition alone is not cytotoxic for MM cells
- β_5/β_2 co-inhibition is the most effective in PI-sensitive and PI-resistant MM
- From the available PI, only high-dose carfilzomib provides β_5/β_2 co-inhibition

Proteasome Inhibition in Multiple Myeloma: Head-to-Head Comparison of Currently Available Proteasome Inhibitors

Andrej Besse,^{1,3} Lenka Besse,^{1,3,4,*} Marianne Kraus,¹ Max Mendez-Lopez,¹ Jürgen Bader,¹ Bo-Tao Xin,² Gerjan de Bruin,² Elmer Maurits,² Herman S. Overkleeft,² and Christoph Driessen¹

¹Experimental Oncology and Hematology, Department of Oncology and Hematology, Cantonal Hospital St. Gallen, Rorschacher Strasse 95, St. Gallen 9007, Switzerland

²Gorlaeus Laboratories, Leiden Institute of Chemistry and Netherlands Proteomics Centre, 2333 CC Leiden, the Netherlands

³These authors contributed equally

⁴Lead Contact

*Correspondence: lenka.besse@kssg.ch or lenka.kubiczek@gmail.com

<https://doi.org/10.1016/j.chembiol.2018.11.007>

SUMMARY

Proteasome inhibitors (PIs) are a backbone of multiple myeloma (MM) therapy. The proteasome harbors six proteolytically active subunits ($\beta 1$, $\beta 2$, $\beta 5$), while $\beta 5$ was identified as rate-limiting and is a primary target of clinically available PIs. The most effective pattern of subunit inhibition provided by these PIs for cytotoxic activity in MM is unknown. A head-to-head comparison of clinically available PIs shows that in the clinically relevant setting only the co-inhibition of $\beta 1$ or $\beta 2$ with $\beta 5$ activity achieves meaningful functional proteasome inhibition and cytotoxicity, while the selective $\beta 2/\beta 5$ inhibition of both constitutive and immunoproteasome is the most cytotoxic. In the long-term setting, selective inhibition of $\beta 5$ subunit is sufficient to induce cytotoxicity in PI-sensitive, but not in PI-resistant MM, and the $\beta 5/\beta 2$ co-inhibition is the most cytotoxic in PI-resistant MM. These results give a rational basis for selecting individual PIs for the treatment of MM.

INTRODUCTION

Proteasome inhibitors (PIs) have improved the survival of patients with multiple myeloma (MM) and represent a backbone of current MM therapy in all treatment phases (Moreau et al., 2012). The first-in-class, reversibly binding peptide boronate-based PI bortezomib (Velcade) (BTZ) has been initially approved for relapsed/refractory MM (Kane et al., 2003) and soon after moved also to the frontline setting (Kouroukis et al., 2014). The second-generation, irreversibly binding peptide epoxyketone-based PI carfilzomib (Kyprolis) (CFZ) has been developed mainly to overcome intrinsic or acquired resistance and off-target toxicity of BTZ (Arastu-Kapur et al., 2011). Currently a third PI, the boronate-based, orally available ixazomib (Ninlaro), is approved in relapsed/refractory MM (Al-Salama et al., 2017). Additional PIs are under clinical investigation, such as

the epoxyketone-based PI oprozomib, the boronate-based PI delanzomib, and the irreversibly proteasome binding β -lactone PI marizomib (Rajan and Kumar, 2016; Vogl et al., 2017).

MM cells produce vast amounts of secretory protein and therefore heavily rely on proper proteasome function (Laubach et al., 2011). Proteasome inhibition in MM disrupts the equilibrium between protein production and disposal of misfolded or non-functional protein, which leads to proteotoxic stress, excess activation of the unfolded protein response, and ultimately apoptosis (Obeng et al., 2006). The 26S proteasome is a large multi-catalytic protein complex composed of the 19S regulatory particle and 20S core particle; the core particle is made of two outer α rings and two inner β rings (Levine and Kroemer, 2008). Each of the β rings contains three individual proteolytic subunits with distinct substrate specificity and activity ($\beta 5$: chymotrypsin-like; $\beta 2$: trypsin-like; $\beta 1$: caspase-like) (Ciechanover, 2005). These subunits of the so-called constitutive (c) proteasome can be replaced by respective immunoproteasome (i) subunits $\beta 1i$, $\beta 2i$, and $\beta 5i$ in immune cells (Huber et al., 2012), where they shape the repertoire of antigenic peptides presented by major histocompatibility complex class I (Rock et al., 2002).

The biological and functional significance of the six different individual proteasome subunits is poorly understood. The $\beta 5$ subunit of the proteasome was initially identified as the rate-limiting protease for proteasomal protein turnover based on the individual genetic knockdown of the proteolytically active protein domains of the constitutive proteasome in yeast (Heinemeyer et al., 1997; Arendt and Hochstrasser, 1997; Groll et al., 1999). Consequently, all PIs clinically available for MM therapy by design target the $\beta 5$ subunit of the constitutive proteasome and immunoproteasome (Kubiczkova et al., 2014; Kisselev et al., 2012). Further work showed that the co-inhibition of $\beta 1$ or $\beta 2$ subunits sensitizes MM cells for treatment with CFZ or BTZ (Mirabella et al., 2011; Kraus et al., 2015). Only recently chemical tools became available that allow selective manipulation and monitoring of the activity of each individual proteolytic subunit (de Bruin et al., 2016). Using these tools, it became evident that all $\beta 5$ -targeted PIs in fact lose their subunit selectivity at higher concentrations and that they co-inhibit either $\beta 1$ and/or $\beta 2$ type of proteasome subunits. These co-inhibition patterns differ between the individual PIs (de Bruin et al., 2016;

Kraus et al., 2015). The functional and biological significance of the different co-inhibitory patterns of the available PI drugs is unknown.

Understanding the functional significance of the different co-inhibitory patterns of PIs may help to explain differential activity and toxicity observed during treatment with different entities or different doses of PIs in head-to-head comparisons. The latter at present yields puzzling results: CFZ is superior or not to BTZ in clinical trials ENDEAVOR versus CLARION (Dimopoulos et al., 2017a; Facon et al., 2017), a once-weekly high dose of CFZ is more active, but not more toxic than a twice-weekly low dose (A.R.R.O.W. trial) (Moreau et al., 2018), with a similar cumulative dose delivered, while a once-weekly dose of BTZ is similarly active and less toxic than a twice-weekly dose (Brinchen et al., 2010). Comparative clinical trials with ixazomib and CFZ or BTZ are entirely lacking, and we have likewise no direct information about the comparative activity of ixazomib, oprozomib, delanzomib, and marizomib.

In this study we performed a head-to-head comparison of the clinically approved and tested PIs in a setup (1-hr pulse treatment) that resembles the pharmacokinetics of clinical intravenous (i.v.) dosing of PIs (Shabaneh et al., 2013). We determined the inhibition profile of the constitutive proteasome and immunoproteasome under increasing concentrations of PIs and also assessed the duration of the inhibition *in vitro*. Using highly selective inhibitors of individual proteasome subunits, we directly linked the inhibition profile of individual β subunits to functional proteasome inhibition and cytotoxicity in MM cells, and demonstrate the $\beta 5c/i$ and $\beta 2c/i$ co-inhibition, which is exclusively achieved by CFZ, at high dose levels is the most effective proteasome inhibition profile in MM, which is also able to overcome BTZ and CFZ resistance. The *in vitro* data are complemented by the proteasome subunit-inhibition profile of boronates and epoxyketone-based drugs after i.v. and intraperitoneal (i.p.) injection *in vivo*.

RESULTS

Side-by-Side Comparison of Clinically Available Proteasome Inhibitors in Viable MM Cells

We performed side-by-side comparison of the clinically available PIs by simultaneous assessment of proteasome activity, functional evaluation of proteasomal proteolysis, and cell death in MM cells. To directly account for functional proteasomal proteolysis we quantified the accumulation of proteasome substrate protein upon proteasome inhibition, using AMO-1 cells equipped with Ub^{-G76V}-GFP, a ubiquitin-fusion degradation substrate that builds up an intracellular fluorescence signal upon functional inhibition of the proteasomal proteolysis pathway. This was complemented by the use of fluorescence-labeled, proteasome activity-based chemical probes (ABP) that allow individual visualization of the activity state of the proteolytic $\beta 1$, $\beta 2$, and $\beta 5$ subunits, as well as a cytotoxicity assay. Cells were treated with increasing doses of proteasome-inhibiting drugs for a 1-hr pulse, followed by removal of the drug, which resembles pharmacokinetic exposure of the drugs during clinical i.v. dosing (Shabaneh et al., 2013). We observed that a 50% inhibition of $\beta 5c/i$ activity was already achieved with BTZ and marizomib at 10 nM concentration, whereas delanzomib required 30 nM, CFZ 100 nM, and

ixazomib and oprozomib 1,000 nM (Figures 1 and S1). More strikingly, we observed qualitative differences in the co-inhibition of $\beta 1$ and $\beta 2$ subunits by the different drugs. Marizomib, as expected, already inhibited the complete set of proteasome subunits at 100 nM. Bortezomib showed complete co-inhibition of $\beta 1c/i$ activity at doses inhibiting $\beta 5c/i$; likewise delanzomib co-inhibits $\beta 1c/i$, although at slightly higher doses than $\beta 5c/i$, while ixazomib displays a slightly higher preference for $\beta 1c/i$ over $\beta 5c/i$ subunit. In contrast to BTZ and ixazomib, CFZ is the only approved proteasome inhibitor with significant $\beta 2$ -inhibiting activity; however, this is only achieved at higher doses of the drug. Furthermore, oprozomib, a next-generation orally available epoxyketone-based drug, prevents increase of $\beta 2c/i$ activity at high dose, which only then is connected with cytotoxicity (Figures 1 and S1). Thus for the PIs, significant or even subtotal inhibition of $\beta 5c/i$ activity alone did not affect the degradation rate of Ub^{-G76V}-GFP or cell viability (e.g., BTZ 30 nM, marizomib 10 nM, CFZ 300 nM) or is possible only when there is no increase in the activity of the other proteasome β subunit (oprozomib, 10 μ M). This suggested that inhibition of $\beta 5c/i$ proteasome activity alone is not sufficient for MM cytotoxicity. By contrast, functional inhibition of proteolysis (as observed from the accumulation of Ub^{-G76V}-GFP) occurred only when significant co-inhibition of $\beta 5$ and at least one additional proteasome subunit (either $\beta 1$ or $\beta 2$) was achieved. While for BTZ 100–1,000 nM the functional proteasome inhibition assessed by Ub^{-G76V}-GFP accumulation and cytotoxicity was achieved through combined $\beta 5/\beta 1$ inhibition (without quantitatively affecting $\beta 2$ activity), a similar effect was reached with CFZ 300–3,000 nM through combined $\beta 5/\beta 2$ inhibition (without affecting $\beta 1$ activity). Ixazomib had functionally by far the weakest on-target activity during pulse exposure. With ixazomib, co-inhibition of $\beta 5/\beta 1$ was observed above 1,000 nM, which resulted only in a weak functional inhibition of proteasomal proteolysis at 10,000 nM, insufficient to translate into cytotoxicity.

The Duration of Proteasome Subunit Inhibition Does Not Differ Based on the Chemistry of the Inhibitor

By their chemical nature, epoxyketone-type PIs (CFZ and oprozomib) provide irreversible proteasome inhibition, while peptide boronates (e.g., BTZ and ixazomib) bind to the proteasome in a reversible fashion. This is taken as an argument to predict a superior duration of functional proteasome inhibition for irreversible inhibitors. However, this issue has not been directly addressed in a head-to-head comparison. Toward this aim, we directly compared the duration of $\beta 5c/i$ inhibition after a pulse treatment with the available PIs (Figure 2). To rule out effects of the differential cytotoxicity of the drugs, we compared the drugs at concentrations that lead to a selective inhibition of $\beta 5c/i$ activity in a 1-hr pulse treatment setting. Ixazomib also co-inhibited $\beta 1c/i$, due to its substrate selectivity mentioned above. The recovery of $\beta 5c/i$ was followed over time for 72 hr using ABP. All PIs showed complete inhibition of $\beta 5c/i$ after 1 hr of treatment (median 10% of residual $\beta 5c/i$ activity, minimum 3% for oprozomib, maximum 13% for BTZ, Figure S2). Within 24 hr, the cells in all settings recovered proteasome $\beta 5c/i$ activity to 50% (median 53% of residual $\beta 5c/i$ activity, minimum 44% for oprozomib and maximum 71% for BTZ). Therefore, there is no significant

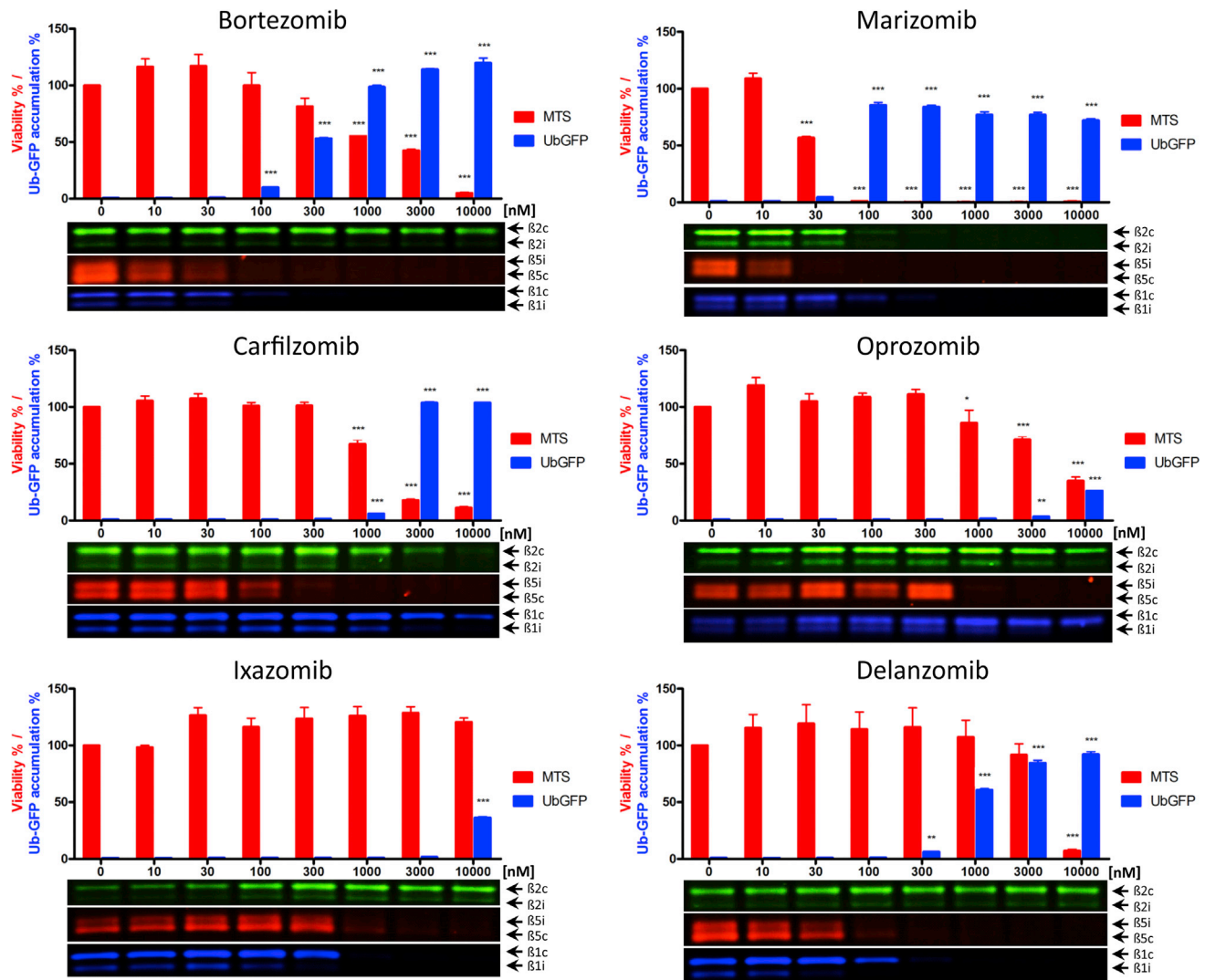


Figure 1. Side-by-Side Comparison of Clinically Approved and Tested Proteasome Inhibitors in AMO-1 Cells Equipped with Ub^{G76V}-GFP Construct

The cells were treated with increasing doses of indicated proteasome inhibitors for 1 hr and then suspended in drug-free medium. Part of the cells was directly lysed for ABP labeling, a second part was incubated for 8 hr for the Ub^{G76V}-GFP fluorescence determination by flow cytometry and third part was seeded for viability determination for 48 hr by MTS assay. For each proteasome inhibitor, subsequent data are represented: gel images of the activity of $\beta 1c/i$ (blue bands), $\beta 2c/i$ (green bands), and $\beta 5c/i$ (red bands) subunits evaluated by ABP labeling and SDS-PAGE, then accumulation of Ub^{G76V}-GFP, represented as blue bars in the graphs, and corresponding cell viability, represented as red bars in the graphs. The Ub^{G76V}-GFP fluorescence and viability data are presented as a mean \pm SD of at least 3 independent experiments, and statistical significance is presented as * $p < 0.05$, ** $p < 0.01$, and *** $p < 0.001$. Gel image is representative of 3 experiments, and quantification of the intensity of the bands is represented in Figure S1.

difference in the duration of proteasome inhibition achieved with the different available drugs.

$\beta 5/\beta 2$ Co-inhibition Is the Most Effective Pattern of Proteasome Inhibition

Given that co-inhibition of non- $\beta 5$ subunits is essential for MM cytotoxicity and that the patterns of this co-inhibition differ between the available PIs, we next aimed to define the most effective pattern of proteasome subunit inhibition to reach maximum functional proteasome inhibition and cytotoxicity in MM cells. Using AMO-Ub^{G76V}-GFP in conjunction with β -subunit-selective PIs of the constitutive proteasome and immuno-

proteasome (described in STAR Methods), we explored the relationship between the different patterns of subunit-selective functional proteasome inhibition, the functional effect on proteasomal protein degradation, and cytotoxicity. This was performed in a similar 1-hr pulse exposure setup as previously with Ub^{G76V}-GFP-AMO-1 cells. Single inhibition of β subunits of constitutive proteasome and immunoproteasome ($\beta 1c/i$, $\beta 2c/i$, $\beta 5c/i$) did not functionally inhibit proteasomal protein turnover and likewise did not lead to cytotoxicity, confirming our observation above. Dual inhibition of $\beta 5c/i$ with $\beta 1c/i$ inhibited proteasome functionally and led to significant cell toxicity. Even more significant functional proteasome inhibition and cytotoxicity

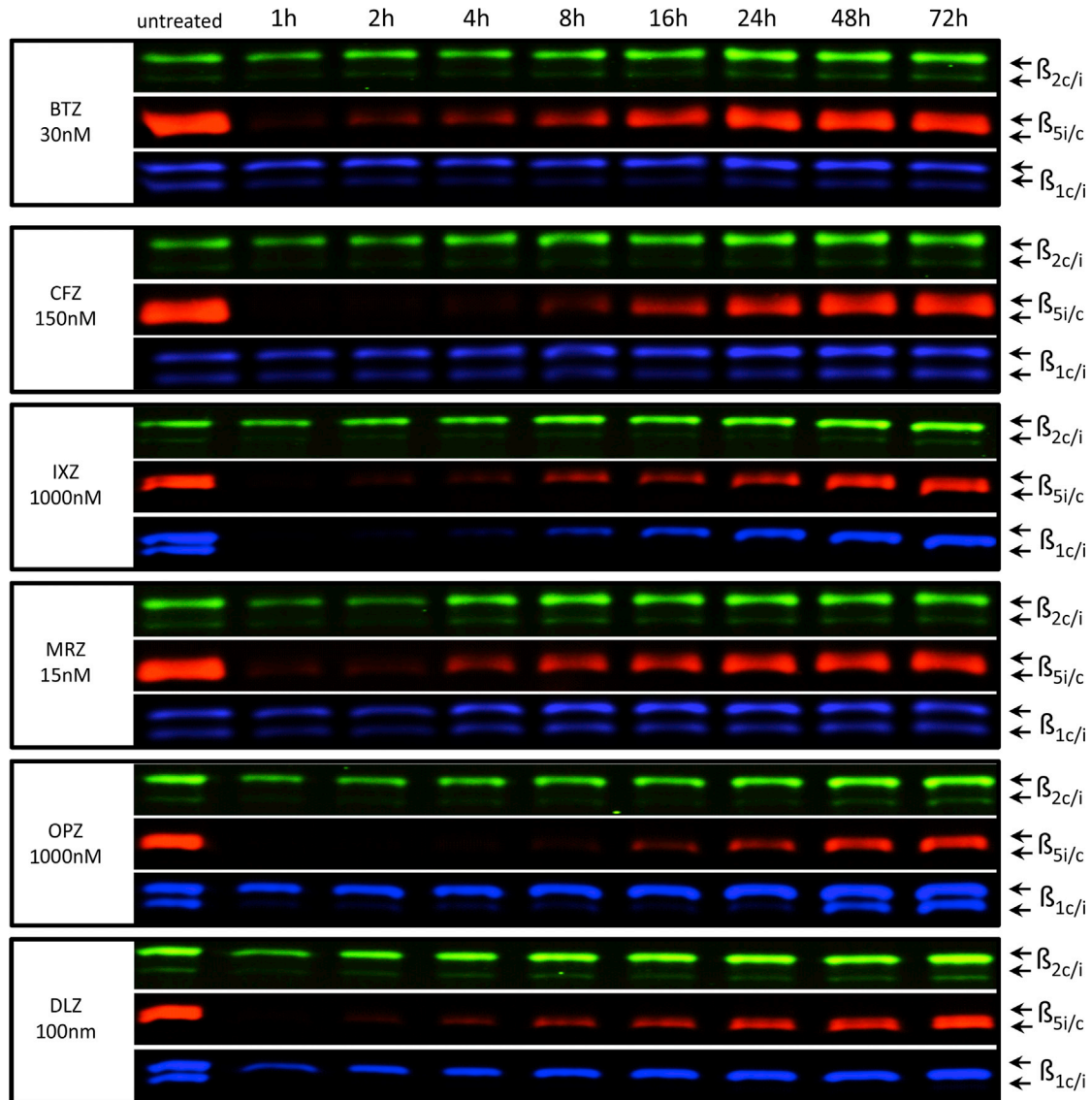


Figure 2. Recovery of Proteasome $\beta 5c/i$ Activity after 1 hr of Pulse Treatment with Indicated Proteasome Inhibitors in AMO-1 Cells

The cells were treated with indicated dose of indicated proteasome inhibitors for 1 hr and then suspended in drug-free medium. Gel images represent the activity of $\beta 1c/i$ (blue bands), $\beta 2c/i$ (green bands), and $\beta 5c/i$ (red bands) subunits after 1 hr of exposure to indicated drug concentration and follow-up of proteasome activity recovery at the indicated time points, evaluated by ABP labeling and SDS-PAGE. BTZ, bortezomib; CFZ, carfilzomib; DLZ, delanzomib; IXZ, ixazomib; MRZ, marizomib; OPZ, oprozomib. The quantification of the intensity of the bands is presented in [Figure S2](#).

were observed when $\beta 5c/i$ with $\beta 2c/i$ subunits were co-inhibited. This combination functionally inhibited proteasomal proteolysis almost as strongly as total proteasome inhibition with $\beta 5c/i$ -, $\beta 2c/i$ -, and $\beta 1c/i$ -selective inhibitors, as deferred from the accumulation of Ub^{-G76V}-GFP ([Figure 3A](#)). Next we analyzed whether selective co-inhibition $\beta 5/\beta 2$ or $\beta 5/\beta 1$ subunits of either the constitutive proteasome or the immunoproteasome (combination of $\beta 5i + \beta 2i$, $\beta 5i + \beta 2c$, $\beta 5c + \beta 2i$, $\beta 5c + \beta 2c$) would likewise induce Ub^{-G76V}-GFP accumulation and cytotoxicity. The results demonstrate that complete inhibition of both species of a subunit (constitutive proteasome and immunoproteasome) is required to achieve a functional effect on protein degradation and cytotoxicity. Thus subunits of the constitutive proteasomes and immu-

noproteasomes are able to take over the protein degradation once the respective corresponding complementary subunit is inhibited ([Figure 3B](#)). Next, we addressed whether the activity of $\beta 5c/i$ and $\beta 2c/i$ subunits is independent from each other or whether the inhibition of one subunit alters the sensitivity of the other subunit for inhibition. Indeed, 5 μM $\beta 2c/i$ -selective inhibitor LU102 was required to induce a sizable reduction in the amount of $\beta 2c/i$ proteasome activity detected in the absence of $\beta 5c/i$ inhibition, while in the presence of $\beta 5c/i$ inhibition a similar effect on $\beta 2c/i$ activity was already reached at 1.25 μM ([Figure 3C](#)). This suggests a better accessibility of the $\beta 2c/i$ subunit for PIs in the presence of $\beta 5c/i$ inhibition, possibly by conformational changes that are induced upon $\beta 5c/i$ inhibition.

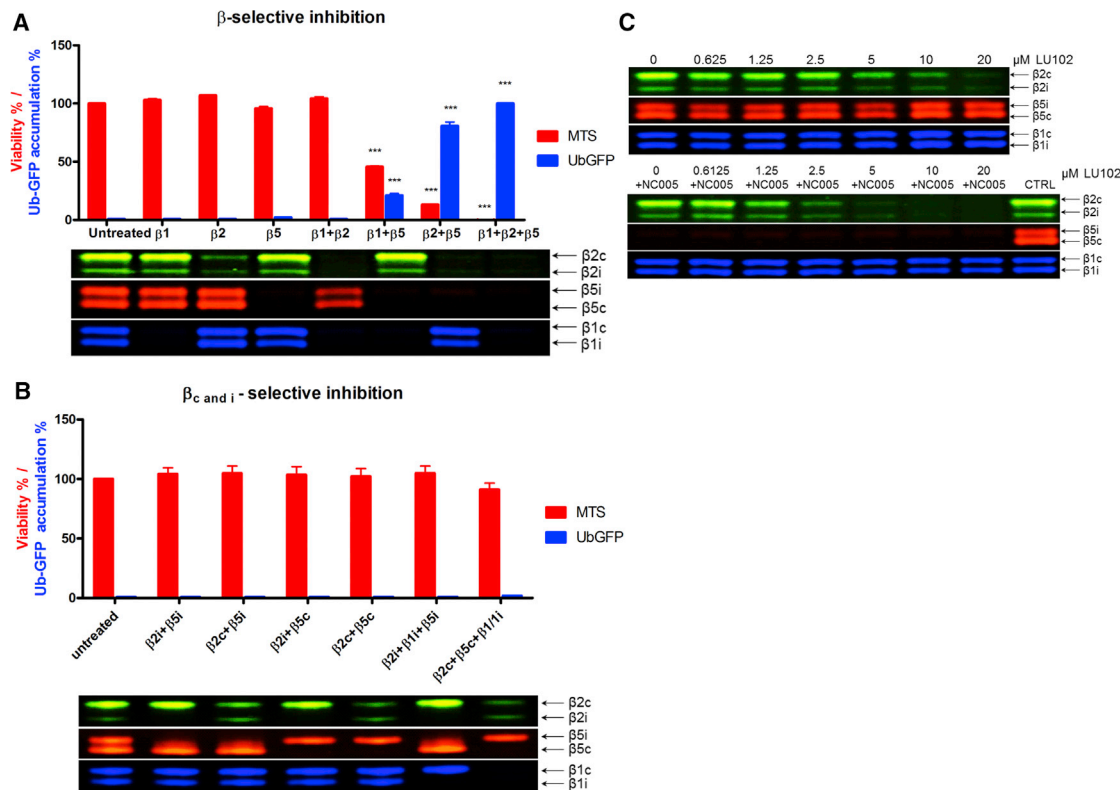


Figure 3. The Most Effective Profile of Proteasome Inhibition Determined in AMO-1 Cells Equipped with Ub^{G76V}-GFP Construct

(A and B) AMO-1 cells were treated with (A) indicated β -subunit-selective inhibitors of different proteasome β subunits of both constitutive and immunoproteasome (c/i) (NC001: $\beta 1c/i$ inhibitor, 10 μM ; LU102: $\beta 2c/i$ inhibitor, 3 μM ; NC005: $\beta 5c/i$ inhibitor, 5 μM) or (B) combination of the selective inhibitors for the β subunits of either constitutive (c) or immunoproteasome (i) (LU001: $\beta 1i$ inhibitor, 2 μM ; NC001: $\beta 1c/i$ inhibitor, 10 μM ; LU002i: $\beta 2i$ inhibitor, 2 μM ; LU002c: $\beta 2c$ inhibitor, 6 μM ; LU015i: $\beta 5i$ inhibitor, 3 μM ; LU025c: $\beta 5c$ inhibitor, 3 μM) for 1 hr, then suspended in drug-free medium. Part of the cells was directly lysed for ABP labeling and SDS-PAGE, a second part was incubated for 8 hr for the Ub^{G76V}-GFP fluorescence determination by flow cytometry, and a third part was seeded for viability determination after 48 hr by MTS assay. The Ub^{G76V}-GFP fluorescence and viability data are presented as a mean \pm SD of 3 independent experiments, statistical significance is presented as *** $p < 0.0001$.

(C) AMO-1 cells were treated with NC005 ($\beta 5c/i$) and LU102 ($\beta 2c/i$) selective inhibitors. In the upper panel, increasing concentrations of LU102 are used to inhibit $\beta 2c/i$ when $\beta 5c/i$ is active, whereas in the lower panel increasing concentrations of LU102 are used to inhibit $\beta 2c/i$ when $\beta 5c/i$ is inhibited with 10 μM NC005. The cells were lysed after 1 hr of exposure to the inhibitors for ABP labeling and SDS-PAGE.

Selective Inhibition of $\beta 2 + \beta 5$, but Not $\beta 1 + \beta 5$, Overcomes Bortezomib and Carfilzomib Resistance in PI-Resistant MM

We next addressed whether combined inhibition of $\beta 5/\beta 2$ subunits is able to overcome PI resistance. Toward this aim, we used BTZ-resistant and CFZ-resistant AMO-1 described earlier (Besse et al., 2018), RPMI8226, L363 cells (aBTZ, aCFZ) (Table 1), in conjunction with 48-hr continuous treatment with PIs *in vitro*. In PI-sensitive cells, already $\beta 5c/i$ inhibition alone led to significant cellular toxicity, while selective $\beta 2$ inhibition had no effect. BTZ-resistant cells are not sensitive to $\beta 5c/i$ -selective proteasome inhibition, consistent with the inhibition profile of BTZ; however, the resistance can be overcome by co-inhibition of $\beta 5$ and $\beta 2c/i$ (Figure 4A), which induces strong synergistic cytotoxicity. Likewise, BTZ resistance of primary malignant plasma cells derived from MM patients could be overcome by combining BTZ with the $\beta 2$ -inhibitor LU102. By contrast, carfilzomib resistant MM cell lines were not sensitive to combined $\beta 5/\beta 2$ proteasome inhibition, although CFZ-resistant primary malignant plasma cells were again significantly sensitive to $\beta 5c/i + \beta 2c/i$ proteasome inhibition (Figures 4B and

4C, additional patients were already shown; Kraus et al., 2015). CFZ-resistant MM cell lines express high activity of ABCB-type drug export proteins (Figure 4D; Besse et al., 2018; Soriano et al., 2016). Epoxyketones, including the selective $\beta 5c/i$ inhibitors used by us, are strong substrates of ABCB-type pumps (Besse et al., 2018). This suggested that the lack of cytotoxic activity of the $\beta 5c/i + \beta 2c/i$ inhibitor combination in CFZ-resistant cells may be due to ABCB1 mediated export of PI, as already published by us (Besse et al., 2018). Indeed, inhibition of ABCB-type efflux pumps by reserpine restored the sensitivity of CFZ-resistant MM cell lines to $\beta 5c/i + \beta 2c/i$ inhibition (Figure 4E). Furthermore, additive $\beta 2$ proteasome inhibition was able to increase the cytotoxicity of all currently available PIs (Figure 5 and Table S1) in cells without strong ABCB-type pump expression (AMOwt, AMOaBTZ), in contrast to cells with high drug efflux activity (AMOaCFZ).

The Proteasome-Inhibiting Activity *In Vivo* Differs between Boronates and Epoxyketones

To address the tissue distribution of the different active subunits of the constitutive proteasome versus immunoproteasome, we

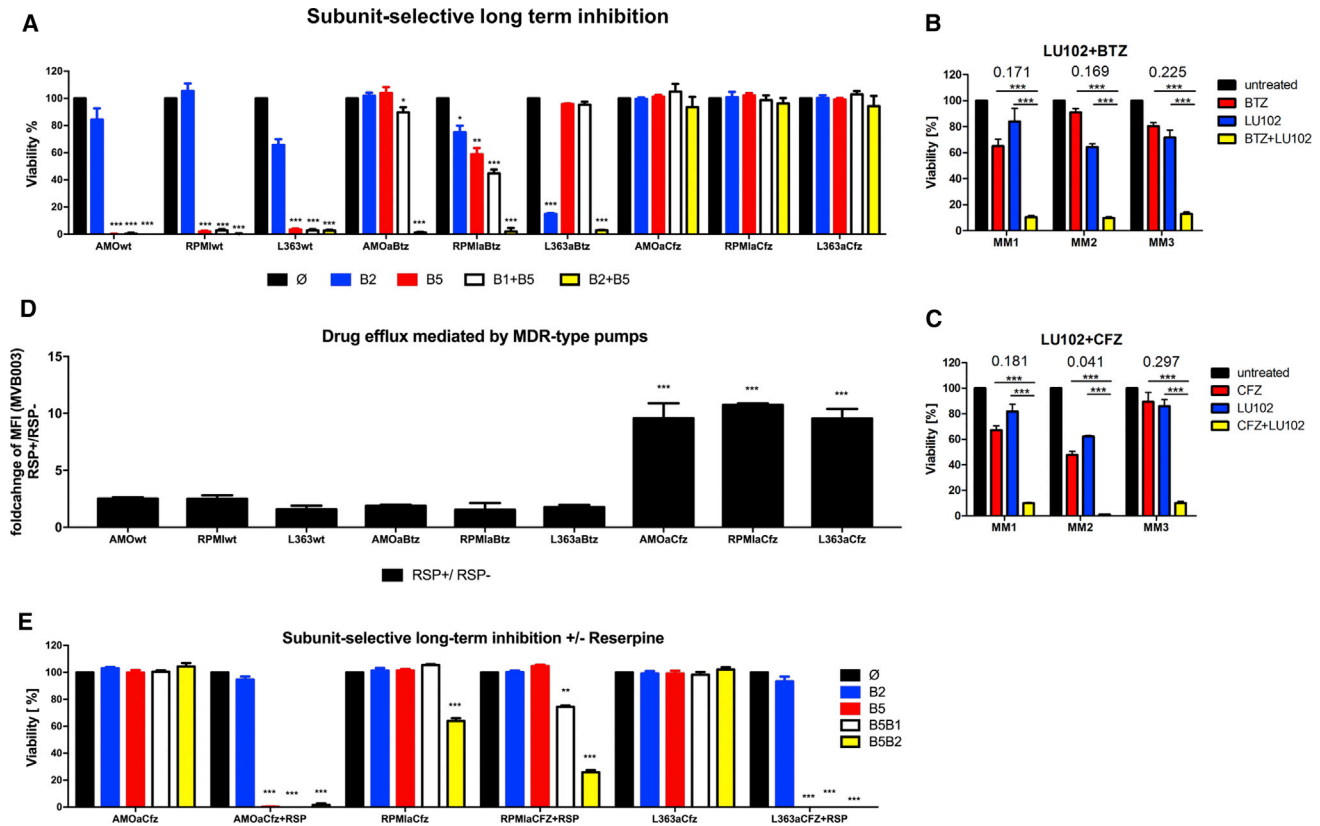


Figure 4. β 5/ β 2 Co-inhibition without or with ABCB Type of Drug Exporters Inhibitors Overcomes Bortezomib and Carfilzomib Resistance in MM

(A) PI-sensitive (wt) and PI-resistant (aBTZ or aCFZ) cell lines were exposed for 48 hr continuously to β -subunit-selective PI or their combination, with subsequent viability determination by MTS. The following concentrations were used: NC001 (β 1c/i inhibitor; 10 μ M), LU102 (β 2c/i inhibitor; 3 μ M), NC005 (β 5c/i inhibitor; 5 μ M).

(B and C) Primary malignant plasma cells from 3 MM patients were exposed for 48 hr to (B) bortezomib (BTZ; MM1: 5 nM, MM2: 2.5 nM, MM3: 5 nM) and (C) carfilzomib (CFZ; MM1 and MM2: 5 nM, MM3: 2.5 nM) alone or in combination with β 2-selective inhibitor LU102 (MM1 and MM2: 10 μ M, MM3: 3.3 μ M). Statistical significance is presented as *** p < 0.001 of respective comparisons obtained by one-way ANOVA with Tukey's post test for each individual MM patient. The coefficient of drug interaction (CDI) is indicated. CDI < 1 indicates a synergistic effect; CDI = 1 indicates an additive effect; CDI > 1 indicates an antagonistic effect.

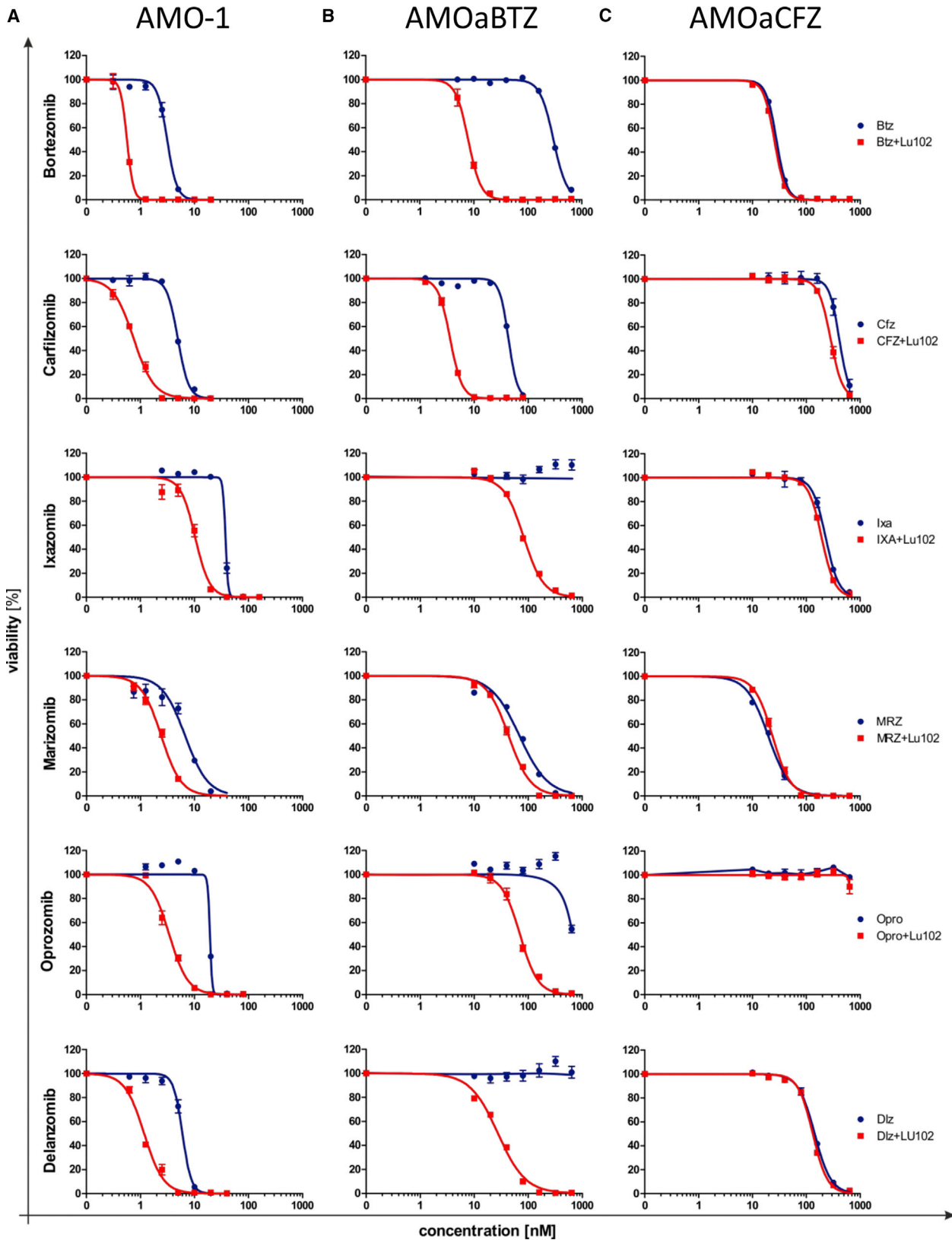
(D) PI-sensitive (wt) and PI-resistant cell lines (aBTZ or aCFZ) were incubated for 3 hr with/without 10 μ M ABCB-type efflux pump inhibitor 10 μ M reserpine (RSP), with subsequent incubation with 1 μ M MVB003, an ABCB1 substrate, for ABCB type of pump activity determination. Median fluorescence intensity (MFI) was measured by flow cytometry and is depicted as a ratio between MVB003 (ABCB1 substrate) labeled and RSP⁺/RSP⁻ (ABCB1 inhibitor) treated cells.

(E) CFZ-resistant cell lines were exposed for 48 hr continuously to β -subunit-selective PIs (drugs and concentrations are indicated in A) or their combination, \pm reserpine, with subsequent viability determination.

The viability and flow-cytometry data for cell lines are presented as a mean \pm SD of at least 3 independent experiments, and statistical significance is presented as * p < 0.05, ** p < 0.01, *** p < 0.001. The IC₅₀ values of PI-resistant cell lines to bortezomib and carfilzomib are presented in Table 1.

performed ABP labeling of extracts from murine organs that have been normalized for equal amounts of total protein (Figures 6A and S3A). The contributions of constitutive proteasome and immunoproteasome markedly differed per organ. While there was an equal distribution between both types in peripheral blood mononuclear cells and bone marrow, immunoproteasome was the dominant species in spleen and lung tissue, while liver and kidney contained mostly constitutive proteasome activity. Immunoproteasome activity was absent from brain lysates. Strikingly, heart tissue contained significantly lower active proteasome per total protein than any other type of organ tested here. This may reflect in part the cardiac vulnerability for high doses of carfilzomib observed in the clinic.

We next asked whether the different inhibitory patterns toward proteasome subunits of BTZ and CFZ would translate into similar differences in the various tissues *in vivo*, either after application that results in high peak plasma levels (*i.v.*, like CFZ) or in an application mode leading to lower peak plasma levels and prolonged exposure (like BTZ, subcutaneous [*s.c.*] in the clinic and *i.p.* in our experimental setup). We therefore treated mice with BTZ (1 mg/kg) and CFZ (4 mg/kg) both *i.v.* and *i.p.* and evaluated proteasome activity 2 hr post treatment. After *i.v.* administration, BTZ significantly inhibited β 5c/i and β 1c/i activity in all studied organs except the brain, whereas CFZ significantly inhibited β 5c/i activity, except for brain and lungs (Figure 6B and S3B). Interestingly, after *i.v.* administration BTZ provided slightly



(legend on next page)

stronger $\beta 5$ -inhibiting activity, despite its lower total dose, compared with CFZ in our setup in all peripheral organs tested, except for the heart. In heart tissue after i.v. injection, CFZ showed a significant reduction of both $\beta 5$ and $\beta 2$ proteasome activity. Clear differences in proteasome inhibition were observed after i.p. administration, where BTZ was as effective as in the i.v. setting, while CFZ failed to inhibit $\beta 5c/i$ to more than 50% in all studied organs apart from the liver (Figures 6C and S3C). Thus, CFZ and BTZ show their different patterns of $\beta 5/\beta 1$ and $\beta 5/\beta 2$ co-inhibition also *in vivo* after systemic administration i.v. or i.p. The pharmacodynamic activity of CFZ after i.p. injection is poor in comparison with BTZ.

DISCUSSION

After the initial approval of BTZ (Kane et al., 2003), new PIs with improved proteasome selectivity, differential subunit-inhibition profiles, and different toxicity profiles are being used and developed (Herndon et al., 2013; Shirley, 2016; Moreau et al., 2012; Kubiczkova et al., 2014). However, the clinical choice between different PIs and their different dosing strategies is based on data from very few clinical head-to-head comparisons in selected settings and/or doses that give partly conflicting results (Brighen et al., 2010; Dimopoulos et al., 2017a; Facon et al., 2017; Moreau et al., 2018).

We here provide a systematic overview of the proteasome inhibition profiles and key functional pharmacodynamic properties of current PI drugs or drug candidates. Our data are consistent with the major clinical results observed to date and may therefore help to guide the future use and dosing of PIs in the next generation of clinical trials.

All PIs by design target the $\beta 5$ proteasome subunit, the key molecular target. Our data show clearly that $\beta 5c/i$ inhibition alone is insufficient to decrease protein breakdown in viable MM cells *in vitro*, after short 1-hr pulse treatment, and lacks cytotoxic activity, in agreement with earlier data (Kisselev et al., 2006). Functional inhibition of proteasomal protein destruction and, hence, cytotoxic activity is only achieved upon co-inhibition of a second β subunit ($\beta 1$ or $\beta 2$), in addition to $\beta 5$ inhibition (either $\beta 5/\beta 1$ or $\beta 5/\beta 2$ co-inhibition) (Weyburne et al., 2017; Kraus et al., 2015). We here show that $\beta 5/\beta 2$ co-inhibition is more effective compared with a $\beta 5/\beta 1$ inhibition profile. While both profiles, $\beta 5/\beta 1$ and $\beta 5/\beta 2$, induce potent cytotoxicity in therapy-sensitive MM cells, $\beta 5/\beta 2$ co-inhibition was more potent and the only inhibition profile that was cytotoxic to proteasome inhibitor-refractory MM cell lines or primary cells. The co-inhibition of $\beta 2$ activity improved the cytotoxic activity of all available proteasome-inhibiting drugs and drug candidates. Interestingly, the chemistry of the PI warhead (exopyketone, β -lactone, or boronate) did not significantly affect the duration of functional proteasome inhibition, consistent with the very slow off-rate of, e.g., BTZ (Kisselev et al., 2012), so that differences observed in the clinical efficacy of

different drugs are hardly explained by reversible versus irreversible proteasome binding.

The cytotoxicity and half maximal inhibitory concentration (IC_{50}) values of PIs vary depending on the treatment schedule used *in vitro*. Here, we used a 1-hr pulse treatment setting because it largely resembles the pharmacokinetic profile after i.v. treatment with PIs in the clinic. This pattern does not directly mirror the situation with the oral inhibitors oprozomib and ixazomib as well as with s.c. BTZ. However, the identical setup used here for each drug allows their direct comparison.

Peptide boronates (BTZ, ixazomib, delanzomib) show a $\beta 5/\beta 1$ proteasome inhibition pattern. CFZ achieves $\beta 5$ inhibition at relatively low concentrations (100 nM in a 1-hr pulse experiment), but is unique in that it is the only PI that induces a dose-dependent co-inhibition of $\beta 2$ activity over a relatively wide concentration range (from 1 μM to 10 μM). The approved dose of 27 mg/m² CFZ results in a 1.79 μM C_{max} , whereas the 56-mg/m² dose given as 30-min infusion translates to a 2.89 μM concentration (Papadopoulos et al., 2015). Thus it is plausible from our data that a 27-mg/m² dosing of CFZ has only very weak $\beta 2$ co-inhibiting activity, because it is at the low end of the concentration range that induces $\beta 2$ co-inhibition (insufficient $\beta 2$ co-inhibition). This is consistent with an inhibitory effect on protein destruction and cytotoxic activity that is comparable with BTZ. High doses of CFZ (56 mg/m² and higher), however, lead to significant $\beta 5/\beta 2$ co-inhibition, which is more potent than $\beta 5/\beta 1$ co-inhibition (Figures 1 and 3). The results from clinical head-to-head comparisons of BTZ and CFZ in MM are consistent with the interpretation that high doses of CFZ are superior to BTZ (ENDEAVOR study, $\beta 5/\beta 2$ inhibition superior to $\beta 5/\beta 1$ inhibition) (Dimopoulos et al., 2016, 2017a), and once-weekly high doses of CFZ are superior to low doses of CFZ (sufficient $\beta 2$ co-inhibition superior to insufficient $\beta 2$ co-inhibition, A.R.R.O.W. trial) (Moreau et al., 2018). On the other hand the standard-dose twice-weekly CFZ, is not more effective than BTZ ($\beta 5/\beta 1$ co-inhibition versus $\beta 5$ inhibition with insufficient $\beta 2$ co-inhibition; CLARION trial) (Facon et al., 2017).

Given that the degree of $\beta 2$ co-inhibition largely determines effective inhibition of protein turnover and cell death (Figure 3A), it appears plausible that it also determines on-target toxicity in non-myeloma cells *in vivo*. The relatively wide dose range over which the increasing $\beta 2$ inhibition activity of CFZ is observed makes it easier to safely titrate the $\beta 2$ -inhibition level (and CFZ dose) to the maximum tolerated level in the clinic. By contrast, marizomib, the only other drug with significant $\beta 2$ -inhibiting activity, shows $\beta 2$ co-inhibition only in a very narrow concentration window between 30 and 100 nM. This feature may make it more difficult to reach a safe $\beta 5/\beta 2$ co-inhibiting dosing with this drug.

Our data show that the heart contains exceptionally low amounts of active proteasome species per microgram of protein (Figure 6), and the i.v. application of CFZ *in vivo* results in a particularly potent inhibition of cardiac $\beta 5/\beta 2$ compared with, e.g., lung tissue, i.v. application of BTZ, or i.p. application of CFZ. This special combination of highly effective inhibitory

Figure 5. Dose-Response Curves of Proteasome Inhibitor-Sensitive and -Resistant Cells to Different Proteasome Inhibitors in Monotherapy or in Combination with $\beta 2$ -Selective Inhibitor

(A–C) (A) AMO-1 PI-sensitive, (B) AMOaBTZ, and (C) AMOaCFZ were exposed for 48 hr to increasing concentrations of clinically available proteasome inhibitors alone or in combination with 3 μM $\beta 2c/i$ -selective inhibitor LU102. BTZ, bortezomib; CFZ, carfilzomib; DLZ, delanzomib; IXZ, ixazomib; MRZ, marizomib; OPZ, oprozomib. IC_{50} values for all proteasome inhibitors as single drugs or in combination with LU102 are presented in Table S1.

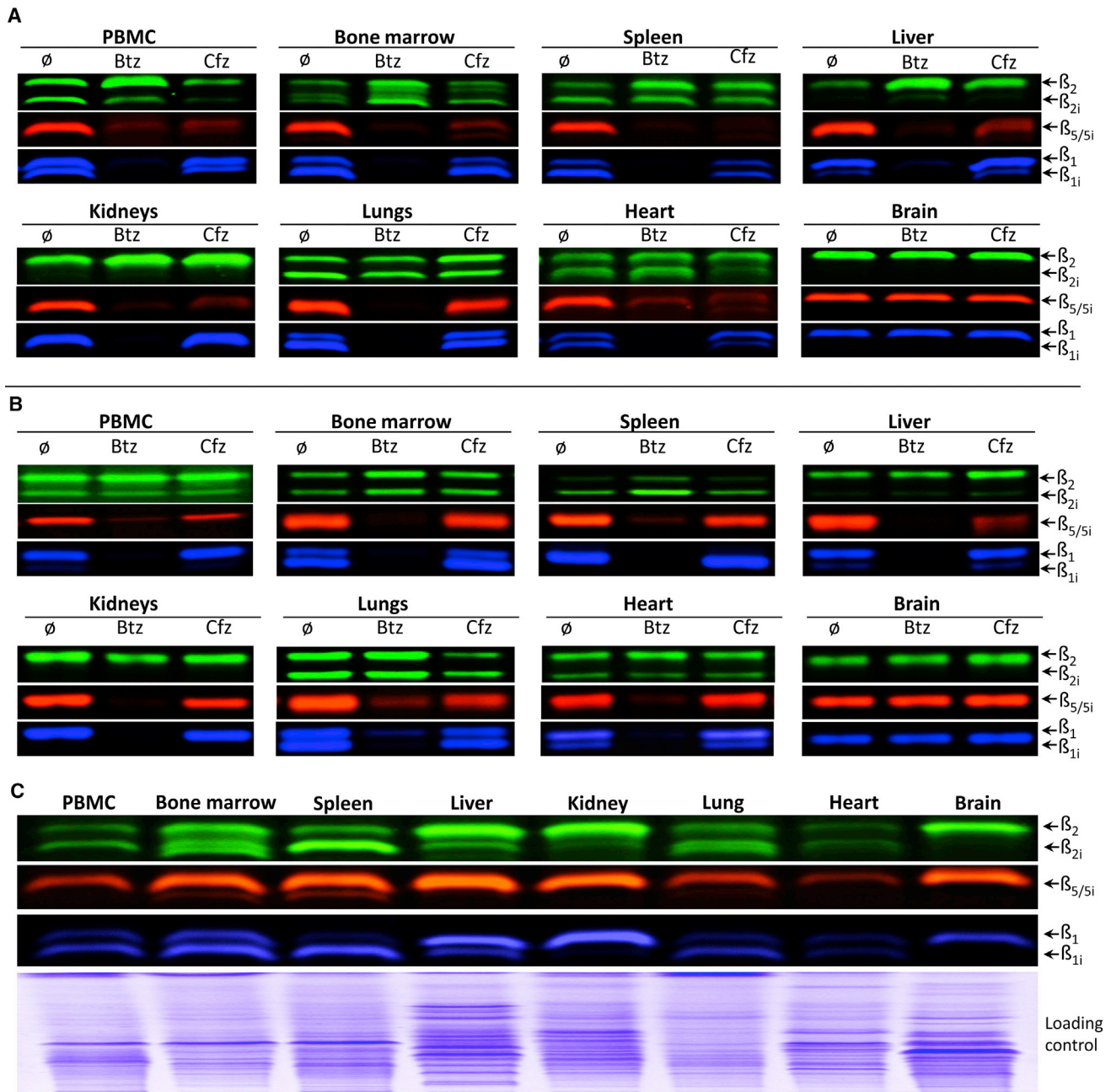


Figure 6. Pharmacodynamic Activity of Bortezomib and Carfilzomib after i.v. and i.p. Administration

(A and B) Basal proteasome activity determined in different mouse organs by ABP labeling and SDS-PAGE (A). Organ processing is described in STAR Methods. (B) Biodistribution and inhibition profile of bortezomib (1 mg/kg) and carfilzomib (4 mg/kg) in different organs from mice 2 hr after i.v. administration of the drugs. (C) Biodistribution and inhibition profile of bortezomib (1 mg/kg) and carfilzomib (4 mg/kg) in different organs from mice 2 hr after i.p. administration of the drugs. The organs were processed; cells were lysed, labeled with ABP, and proteasome subunits were separated by SDS-PAGE. Green bands indicate $\beta_{2c/i}$ subunit activity, red bands indicate $\beta_{5c/i}$ subunit activity, and blue bands indicate $\beta_{1c/i}$ subunit activity. The quantification of the intensity of the bands for each panel is presented in Figure S3.

pattern (β_5/β_2), tissue distribution, and low cardiac proteasomal capacity may serve as a mechanistic basis for the cardiac toxicity of PIs, and especially CFZ (Dimopoulos et al., 2017b).

β_5/β_2 co-inhibition with boronate-based drugs was effective in resistant cell lines and primary patient samples, despite the presence of *PSMB5* mutations in the cell lines, which has

recently been confirmed also in patient samples (Barrio et al., 2018). This co-inhibition with epoxyketone-based inhibitors, which are strong substrates for ABCB-type drug transporters, was not effective in CFZ-resistant cell lines *in vitro* due to high functional expression of ABCB-type transporters (Besse et al., 2018; Soriano et al., 2016). Likewise, solid tumors or circulating

Table 1. Characteristics of Proteasome Inhibitor-Sensitive and -Resistant Cell Lines

Cell Line	IC ₅₀ BTZ (nM)	IC ₅₀ CFZ (nM)	PSMB5 Status
AMO-1	4.009	4.798	wt
RPMI-8226	5.259	10.81	wt
L363	5.595	5.156	wt
AMOaBTZ	178.2	25.34	A310G (Met45Val) heterozygous
RPMIaBTZ	147.4	38.33	G322A (Ala49Thr)
L363aBTZ	151.3	31.78	G322A (Ala49Thr)
AMOaCFZ	18.52	195.7	wt
RPMIaCFZ	167.4	531.5	wt
L363aCFZ	17.21	253.6	wt

IC₅₀ values for proteasome inhibitors bortezomib (BTZ) and carfilzomib (CFZ) in proteasome inhibitor-sensitive (AMO-1, RPMI-8226 ad L363) and proteasome inhibitor-resistant cells (cells resistant to bortezomib: AMOaBTZ, RPMIaBTZ, L363aBTZ; cells resistant to carfilzomib: AMOaCFZ, RPMIaCFZ, L363aCFZ) used in Figures 4A, 4D, 4E, and 5; and mutation status within the active site of PSMB5 subunit. wt, wild-type. Mutations are presented as respective substitutions on gene and protein level (in parentheses).

MM plasma cells with high expression of ABCB1 are not sensitive to CFZ even in high doses (Abt et al., 2018; Pilarski et al., 1997). Inhibition of ABCB1-type transporters is able to sensitize the CFZ-resistant cells to $\beta 5/\beta 2$ inhibition and likewise to CFZ (Besse et al., 2018; Abt et al., 2018; Soriano et al., 2016). Several reports showed effective $\beta 5/\beta 2$ proteasome inhibition by two independent drugs, or by one single molecule, such as CFZ or syringolin analog syringolog-1 (Kraus et al., 2015; Weyburne et al., 2017; Yoshida et al., 2018). We here show that $\beta 5/\beta 2$ dual inhibition using two selective inhibitors is more effective than one bispecific inhibitor, as lower doses of $\beta 2$ inhibitor are needed to fully inhibit $\beta 2$ activity when the $\beta 5$ site is inactive, compared with the setting when $\beta 5$ is active. This is likely possible due to allosteric regulation of active proteasome subunits (Kisselev et al., 1999). The use of two selective inhibitors allows for lower dose of the inhibitors to be used with the same effect on proteasome subunit inhibition, which may translate into fewer side effects; moreover, it allows a sequential dosing of the therapy, which may minimize the acute toxicity (Dimopoulos et al., 2016).

Next, our data (Figure 3B) largely rule out that selective immunoproteasome inhibitors can be used in monotherapy to achieve proteotoxic stress and cytotoxicity in cell types that co-express the immunoproteasome together with the constitutive proteasome, such as myeloma. Selective immunoproteasome $\beta 5$ inhibitors may, however, have a cytotoxic potential to eliminate cells that exclusively express the immunoproteasome, such as pediatric acute lymphoblastic leukemia or autoimmune diseases, or even in MM when combined with other subunits inhibitors such as $\beta 2$ (Niewerth et al., 2016; Basler et al., 2015; Downey-Kopy-scinski et al., 2018).

SIGNIFICANCE

Proteasome inhibitors are a backbone of multiple myeloma therapy. We herein provide comprehensive side-by-side

direct comparison of the pharmacodynamic activity of the proteasome inhibitors that are clinically available. Our results show that selective inhibition of the primary pharmaceutical target, the $\beta 5$ subunit, has no functional effect in myeloma in a short-term exposure setting. Proteotoxic stress and cytotoxicity is set only upon co-inhibition of either $\beta 5/\beta 1$ species or $\beta 5/\beta 2$ species. The $\beta 5/\beta 2$ inhibitory pattern has higher functionally proteasome-inhibiting and cytotoxic activity than the $\beta 5/\beta 1$ pattern. Proteasome inhibitor resistance could be overcome exclusively by $\beta 5/\beta 2$ inhibition. Full $\beta 5/\beta 2$ -type of proteasome inhibition is reached by carfilzomib only at higher concentrations, and not by bortezomib or low doses of carfilzomib, consistent with the results from clinical head-to-head comparisons. We conclude that co-inhibition of $\beta 5/\beta 2$ is a functionally more efficient mode of proteasome inhibition than co-inhibition of $\beta 5/\beta 1$. This is likely to translate into a higher clinical effectiveness of $\beta 5/\beta 2$ inhibition with, e.g., carfilzomib versus bortezomib in situations where maximum functional proteasome inhibition is the aim, and supports the use of carfilzomib at doses of 56 mg/m² or 70 mg/m² as opposed to lower doses. However, on-target toxicity in nonrelated organs, in particular cardiac toxicity, may also well be more closely associated with this more effective mode of proteasome inhibition, and needs to be addressed and better understood.

STAR★METHODS

Detailed methods are provided in the online version of this paper and include the following:

- KEY RESOURCES TABLE
- CONTACT FOR REAGENT AND RESOURCE SHARING
- EXPERIMENTAL MODEL AND SUBJECT DETAILS
 - Cell Lines
 - Primary Cells
 - Balb/c Mice
- METHOD DETAILS
 - Proteasome Subunit Selective Inhibitors
 - Activity-Based Probes Labelling
 - In Vivo Drug Distribution
 - Organs and Single Cells Isolation
 - Generation of AMO-1 Ub^{-G76V}-GFP Cells
 - Flow Cytometry
 - Assessment of Cell Viability
- QUANTIFICATION AND STATISTICAL ANALYSIS

SUPPLEMENTAL INFORMATION

Supplemental Information includes three figures and one table and can be found with this article online at <https://doi.org/10.1016/j.chembiol.2018.11.007>.

ACKNOWLEDGMENTS

The authors would like to thank Bogdan I. Florea for the support. The research was supported by Krebsliga Schweiz (KFS-3567-02-2015), Wilhelm Sander-Stiftung (2016.104.1), Onyx/Amgen translational research support, Promedica Stiftung (1438/M), and Swiss National Foundation grant SNF 310030_182492.

AUTHOR CONTRIBUTIONS

A.B. and L.B. performed the experiments, analyzed the data, and designed and wrote the manuscript; M.K. was responsible for primary MM experiments and data; M.M.-L. helped with *in vivo* experiments; J.B. adapted the cells to proteasome inhibitors; B.-T.X., G.d.B., and E.M. synthesized the ABP and selective inhibitors; H.S.O. provided the chemicals; C.D. designed and critically revised the manuscript.

DECLARATION OF INTERESTS

The authors declare no competing interests.

Received: August 28, 2018

Revised: October 18, 2018

Accepted: November 12, 2018

Published: January 3, 2019

REFERENCES

- Abt, D., Besse, A., Sedlarikova, L., Kraus, M., Bader, J., Silzle, T., Vodinska, M., Slaby, O., Schmid, H.P., Engeler, D.S., et al. (2018). Improving the efficacy of proteasome inhibitors in the treatment of renal cell carcinoma by combination with the human immunodeficiency virus (HIV)-protease inhibitors lopinavir or nelfinavir. *BJU Int.* **121**, 600–609.
- Al-Salama, Z.T., Garnock-Jones, K.P., and Scott, L.J. (2017). Ixazomib: a review in relapsed and/or refractory multiple myeloma. *Target Oncol.* **12**, 535–542.
- Amend, S.R., Valkenburg, K.C., and Pienta, K.J. (2016). Murine hind limb long bone dissection and bone marrow isolation. *J. Vis. Exp.* <https://doi.org/10.3791/53936>.
- Arastu-Kapur, S., Anderl, J.L., Kraus, M., Parlati, F., Shenk, K.D., Lee, S.J., Muchamuel, T., Bennett, M.K., Driessen, C., Ball, A.J., and Kirk, C.J. (2011). Nonproteasomal targets of the proteasome inhibitors bortezomib and carfilzomib: a link to clinical adverse events. *Clin. Cancer Res.* **17**, 2734–2743.
- Arendt, C.S., and Hochstrasser, M. (1997). Identification of the yeast 20S proteasome catalytic centers and subunit interactions required for active-site formation. *Proc. Natl. Acad. Sci. U S A* **94**, 7156–7161.
- Barrio, S., Stuhmer, T., Da-Via, M., Barrio-Garcia, C., Lehnert, N., Besse, A., Cuenca, I., Garitano-Trojaola, A., Fink, S., Leich, E., et al. (2018). Spectrum and functional validation of PSMB5 mutations in multiple myeloma. *Leukemia*. <https://doi.org/10.1038/s41375-018-0216-8>.
- Basler, M., Mundt, S., Bitzer, A., Schmidt, C., and Groettrup, M. (2015). The immunoproteasome: a novel drug target for autoimmune diseases. *Clin. Exp. Rheumatol.* **33**, S74–S79.
- Besse, A., Stolze, S.C., Rasche, L., Weinhold, N., Morgan, G.J., Kraus, M., Bader, J., Overkleeft, H.S., Besse, L., and Driessen, C. (2018). Carfilzomib resistance due to ABCB1/MDR1 overexpression is overcome by nelfinavir and lopinavir in multiple myeloma. *Leukemia* **32**, 391–401.
- Bringhen, S., Larocca, A., Rossi, D., Cavalli, M., Genuardi, M., Ria, R., Gentili, S., Patriarca, F., Nozzoli, C., Levi, A., et al. (2010). Efficacy and safety of once-weekly bortezomib in multiple myeloma patients. *Blood* **116**, 4745–4753.
- Britton, M., Lucas, M.M., Downey, S.L., Screen, M., Pletnev, A.A., Verdoes, M., Tokhunts, R.A., Amir, O., Goddard, A.L., Pelphey, P.M., et al. (2009). Selective inhibitor of proteasome's caspase-like sites sensitizes cells to specific inhibition of chymotrypsin-like sites. *Chem. Biol.* **16**, 1278–1289.
- Ciechanover, A. (2005). Proteolysis: from the lysosome to ubiquitin and the proteasome. *Nat. Rev. Mol. Cell Biol.* **6**, 79–87.
- Dantuma, N.P., Lindsten, K., Glas, R., Jellne, M., and Masucci, M.G. (2000). Short-lived green fluorescent proteins for quantifying ubiquitin/proteasome-dependent proteolysis in living cells. *Nat. Biotechnol.* **18**, 538–543.
- de Bruin, G., Huber, E.M., Xin, B.T., van Rooden, E.J., Al-Ayed, K., Kim, K.B., Kisselev, A.F., Driessen, C., van der Stelt, M., van der Marel, G.A., et al. (2014). Structure-based design of beta1i or beta5i specific inhibitors of human immunoproteasomes. *J. Med. Chem.* **57**, 6197–6209.
- de Bruin, G., Xin, B.T., Kraus, M., van der Stelt, M., van der Marel, G.A., Kisselev, A.F., Driessen, C., Florea, B.I., and Overkleeft, H.S. (2016). A set of activity-based probes to visualize human (immuno)proteasome activities. *Angew. Chem. Int. Ed.* **55**, 4199–4203.
- Dimopoulos, M.A., Goldschmidt, H., Niesvizky, R., Joshua, D., Chng, W.J., Oriol, A., Orlowski, R.Z., Ludwig, H., Facon, T., Hajek, R., et al. (2017a). Carfilzomib or bortezomib in relapsed or refractory multiple myeloma (ENDEAVOR): an interim overall survival analysis of an open-label, randomised, phase 3 trial. *Lancet Oncol.* **18**, 1327–1337.
- Dimopoulos, M.A., Moreau, P., Palumbo, A., Joshua, D., Pour, L., Hajek, R., Facon, T., Ludwig, H., Oriol, A., Goldschmidt, H., et al. (2016). Carfilzomib and dexamethasone versus bortezomib and dexamethasone for patients with relapsed or refractory multiple myeloma (ENDEAVOR): a randomised, phase 3, open-label, multicentre study. *Lancet Oncol.* **17**, 27–38.
- Dimopoulos, M.A., Roussou, M., Gavriatopoulou, M., Psimenou, E., Ziogas, D., Eleutherakis-Papaikovou, E., Fotiou, D., Migkou, M., Kanellias, N., Panagiotidis, I., et al. (2017b). Cardiac and renal complications of carfilzomib in patients with multiple myeloma. *Blood Adv.* **1**, 449–454.
- Downey-Kopyscinski, S., Daily, E.W., Gautier, M., Bhatt, A., Florea, B.I., Mitsiades, C.S., Richardson, P.G., Driessen, C., Overkleeft, H.S., and Kisselev, A.F. (2018). An inhibitor of proteasome beta2 sites sensitizes myeloma cells to immunoproteasome inhibitors. *Blood Adv.* **2**, 2443–2451.
- Facon, T., Lee, J.H., Moreau, P., Niesvizky, R., Dimopoulos, M.A., Hajek, R., Osman, M., Aggarwal, S., Klippel, Z., and San Miguel, J. (2017). Phase 3 study (CLARION) of carfilzomib, melphalan, prednisone (KMP) v bortezomib, melphalan, prednisone (VMP) in newly diagnosed multiple myeloma (NDMM). *Clin. Lymphoma Myeloma Leuk.* **17**, e26–e27.
- Geurink, P.P., van der Linden, W.A., Mirabella, A.C., Gallastegui, N., de Bruin, G., Blom, A.E., Voges, M.J., Mock, E.D., Florea, B.I., van der Marel, G.A., et al. (2013). Incorporation of non-natural amino acids improves cell permeability and potency of specific inhibitors of proteasome trypsin-like sites. *J. Med. Chem.* **56**, 1262–1275.
- Groll, M., Heinemeyer, W., Jager, S., Ullrich, T., Bochtler, M., Wolf, D.H., and Huber, R. (1999). The catalytic sites of 20S proteasomes and their role in subunit maturation: a mutational and crystallographic study. *Proc. Natl. Acad. Sci. U S A* **96**, 10976–10983.
- Heinemeyer, W., Fischer, M., Krimmer, T., Stachon, U., and Wolf, D.H. (1997). The active sites of the eukaryotic 20 S proteasome and their involvement in subunit precursor processing. *J. Biol. Chem.* **272**, 25200–25209.
- Herndon, T.M., Deisseroth, A., Kaminskas, E., Kane, R.C., Koti, K.M., Rothmann, M.D., Habtemariam, B., Bullock, J., Bray, J.D., Hawes, J., et al. (2013). U.S. Food and Drug Administration approval: carfilzomib for the treatment of multiple myeloma. *Clin. Cancer Res.* **19**, 4559–4563.
- Huber, E.M., Basler, M., Schwab, R., Heinemeyer, W., Kirk, C.J., Groettrup, M., and Groll, M. (2012). Immuno- and constitutive proteasome crystal structures reveal differences in substrate and inhibitor specificity. *Cell* **148**, 727–738.
- Kane, R.C., Bross, P.F., Farrell, A.T., and Pazdur, R. (2003). Velcade: U.S. FDA approval for the treatment of multiple myeloma progressing on prior therapy. *Oncologist* **8**, 508–513.
- Kisselev, A.F., Akopian, T.N., Castillo, V., and Goldberg, A.L. (1999). Proteasome active sites allosterically regulate each other, suggesting a cyclical bite-chew mechanism for protein breakdown. *Mol. Cell* **4**, 395–402.
- Kisselev, A.F., Callard, A., and Goldberg, A.L. (2006). Importance of the different proteolytic sites of the proteasome and the efficacy of inhibitors varies with the protein substrate. *J. Biol. Chem.* **281**, 8582–8590.
- Kisselev, A.F., van der Linden, W.A., and Overkleeft, H.S. (2012). Proteasome inhibitors: an expanding army attacking a unique target. *Chem. Biol.* **19**, 99–115.
- Kolodziejek, I., Misas-Villamil, J.C., Kaschani, F., Clerc, J., Gu, C., Krahn, D., Niessen, S., Verdoes, M., Willems, L.I., Overkleeft, H.S., et al. (2011). Proteasome activity imaging and profiling characterizes bacterial effector syringolin A. *Plant Physiol.* **155**, 477–489.

- Kouroukis, T.C., Baldassarre, F.G., Haynes, A.E., Imrie, K., Reece, D.E., and Cheung, M.C. (2014). Bortezomib in multiple myeloma: systematic review and clinical considerations. *Curr. Oncol.* *21*, e573–603.
- Kraus, M., Bader, J., Geurink, P.P., Weyburne, E.S., Mirabella, A.C., Silzle, T., Shabaneh, T.B., van der Linden, W.A., de Bruin, G., Haile, S.R., et al. (2015). The novel beta2-selective proteasome inhibitor LU-102 synergizes with bortezomib and carfilzomib to overcome proteasome inhibitor resistance of myeloma cells. *Haematologica* *100*, 1350–1360.
- Kubiczkova, L., Pour, L., Sedlarikova, L., Hajek, R., and Sevcikova, S. (2014). Proteasome inhibitors - molecular basis and current perspectives in multiple myeloma. *J. Cell. Mol. Med.* *18*, 947–961.
- Laubach, J., Richardson, P., and Anderson, K. (2011). Multiple myeloma. *Annu. Rev. Med.* *62*, 249–264.
- Levine, B., and Kroemer, G. (2008). Autophagy in the pathogenesis of disease. *Cell* *132*, 27–42.
- Li, X., Lin, Z., Zhang, B., Guo, L., Liu, S., Li, H., Zhang, J., and Ye, Q. (2016). beta-elemene sensitizes hepatocellular carcinoma cells to oxaliplatin by preventing oxaliplatin-induced degradation of copper transporter 1. *Sci. Rep.* *6*, 21010.
- Mirabella, A.C., Pletnev, A.A., Downey, S.L., Florea, B.I., Shabaneh, T.B., Britton, M., Verdoes, M., Filippov, D.V., Overkleeft, H.S., and Kisselev, A.F. (2011). Specific cell-permeable inhibitor of proteasome trypsin-like sites selectively sensitizes myeloma cells to bortezomib and carfilzomib. *Chem. Biol.* *18*, 608–618.
- Moreau, P., Mateos, M.V., Berenson, J.R., Weisel, K., Lazzaro, A., Song, K., Dimopoulos, M.A., Huang, M., Zahlten-Kumeli, A., and Stewart, A.K. (2018). Once weekly versus twice weekly carfilzomib dosing in patients with relapsed and refractory multiple myeloma (A.R.R.O.W.): interim analysis results of a randomised, phase 3 study. *Lancet Oncol.* *19*, 953–964.
- Moreau, P., Richardson, P.G., Cavo, M., Orlovski, R.Z., San Miguel, J.F., Palumbo, A., and Harousseau, J.L. (2012). Proteasome inhibitors in multiple myeloma: 10 years later. *Blood* *120*, 947–959.
- Niewerth, D., Kaspers, G.J., Jansen, G., van Meerloo, J., Zweegman, S., Jenkins, G., Whitlock, J.A., Hunger, S.P., Lu, X., Alonzo, T.A., et al. (2016). Proteasome subunit expression analysis and chemosensitivity in relapsed paediatric acute leukaemia patients receiving bortezomib-containing chemotherapy. *J. Hematol. Oncol.* *9*, 82.
- Obeng, E.A., Carlson, L.M., Gutman, D.M., Harrington, W.J., Jr., Lee, K.P., and Boise, L.H. (2006). Proteasome inhibitors induce a terminal unfolded protein response in multiple myeloma cells. *Blood* *107*, 4907–4916.
- Papadopoulos, K.P., Siegel, D.S., Vesole, D.H., Lee, P., Rosen, S.T., Zojwalla, N., Holahan, J.R., Lee, S., Wang, Z., and Badros, A. (2015). Phase I study of 30-minute infusion of carfilzomib as single agent or in combination with low-dose dexamethasone in patients with relapsed and/or refractory multiple myeloma. *J. Clin. Oncol.* *33*, 732–739.
- Pilarski, L.M., Szczepek, A.J., and Belch, A.R. (1997). Deficient drug transporter function of bone marrow-localized and leukemic plasma cells in multiple myeloma. *Blood* *90*, 3751–3759.
- Rajan, A.M., and Kumar, S. (2016). New investigational drugs with single-agent activity in multiple myeloma. *Blood Cancer J.* *6*, e451.
- Rock, K.L., York, I.A., Saric, T., and Goldberg, A.L. (2002). Protein degradation and the generation of MHC class I-presented peptides. *Adv. Immunol.* *80*, 1–70.
- Schindelin, J., Arganda-Carreras, I., Frise, E., Kaynig, V., Longair, M., Pietzsch, T., Preibisch, S., Rueden, C., Saalfeld, S., Schmid, B., et al. (2012). Fiji: an open-source platform for biological-image analysis. *Nat. Methods* *9*, 676–682.
- Shabaneh, T.B., Downey, S.L., Goddard, A.L., Screen, M., Lucas, M.M., Eastman, A., and Kisselev, A.F. (2013). Molecular basis of differential sensitivity of myeloma cells to clinically relevant bolus treatment with bortezomib. *PLoS One* *8*, e56132.
- Shirley, M. (2016). Ixazomib: first global approval. *Drugs* *76*, 405–411.
- Soriano, G.P., Besse, L., Li, N., Kraus, M., Besse, A., Meeuwenoord, N., Bader, J., Everts, B., den Dulk, H., Overkleeft, H.S., et al. (2016). Proteasome inhibitor-adapted myeloma cells are largely independent from proteasome activity and show complex proteomic changes, in particular in redox and energy metabolism. *Leukemia* *30*, 2198–2207.
- van der Linden, W.A., Willems, L.I., Shabaneh, T.B., Li, N., Ruben, M., Florea, B.I., van der Marel, G.A., Kaiser, M., Kisselev, A.F., and Overkleeft, H.S. (2012). Discovery of a potent and highly beta1 specific proteasome inhibitor from a focused library of urea-containing peptide vinyl sulfones and peptide epoxyketones. *Org. Biomol. Chem.* *10*, 181–194.
- Vogl, D.T., Martin, T.G., Vij, R., Hari, P., Mikhael, J.R., Siegel, D., Wu, K.L., Delforge, M., and Gasparetto, C. (2017). Phase I/II study of the novel proteasome inhibitor delanzomib (CEP-18770) for relapsed and refractory multiple myeloma. *Leuk. Lymphoma* *58*, 1872–1879.
- Weyburne, E.S., Wilkins, O.M., Sha, Z., Williams, D.A., Pletnev, A.A., de Bruin, G., Overkleeft, H.S., Goldberg, A.L., Cole, M.D., and Kisselev, A.F. (2017). Inhibition of the proteasome beta2 site sensitizes triple-negative breast cancer cells to beta5 inhibitors and suppresses Nrf1 activation. *Cell Chem. Biol.* *24*, 218–230.
- Yoshida, T., Ri, M., Kanamori, T., Aoki, S., Ashour, R., Kinoshita, S., Narita, T., Totani, H., Masaki, A., Ito, A., et al. (2018). Potent anti-tumor activity of a syringolin analog in multiple myeloma: a dual inhibitor of proteasome activity targeting beta2 and beta5 subunits. *Oncotarget* *9*, 9975–9991.

STAR★METHODS

KEY RESOURCES TABLE

REAGENT or RESOURCE	SOURCE	IDENTIFIER
Chemicals, Peptides, and Recombinant Proteins		
bortezomib (PS-341)	Selleck Chemicals	S1013
carfilzomib (PR-171)	Selleck Chemicals	S2853
marizomib (NPI-0052)	Adipogen	AG-CN2-0444-C100
delanzomib (CEP-18700)	Selleck Chemicals	S1157
oprozomib (ONX0912)	Selleck Chemicals	S7049
ixazomib (MLN9708)	Selleck Chemicals	S2181
LU-001i (β 1i selective inhibitor)	(de Bruin et al., 2014) Leiden University	N/A
NC001 (β 1c/i selective inhibitor)	(van der Linden et al., 2012) Leiden University	N/A
LU-002i (β 2i selective inhibitor)	(de Bruin et al., 2016) Leiden University	N/A
LU-002c (β 2c selective inhibitor)	(de Bruin et al., 2016) Leiden University	N/A
LU-025c (β 5c selective inhibitor)	(de Bruin et al., 2014) Leiden University	N/A
LU-015i (β 5i selective inhibitor)	(de Bruin et al., 2016) Leiden University	N/A
LU-102 (β 2c/i selective inhibitor)	(Geurink et al., 2013) Leiden University	N/A
NC005 (β 5c/i selective inhibitor)	(Britton et al., 2009) Leiden University	N/A
Activity based probes	(de Bruin et al., 2016) Leiden University	N/A
MVB003	(Kolodziejek et al., 2011) Leiden University	N/A
Experimental Models: Cell Lines		
AMO-1	DSMZ	ACC538
RPMI-8226	ATCC	CCL-155
L363	DSMZ	ACC 49
Experimental Model: Organisms/Strains		
Balb/cJ	Jackson laboratories	000651
Critical Commercial Assays		
CellTiter 96® AQueous One Solution	Promega	G3581
MethoCult	StemCell Technologies	H4434
Recombinant DNA		
Ub ^{-G76V} -GFP	(Dantuma et al., 2000)	Addgene plasmid #11941
Software and Algorithms		
FlowJo v10 Software	FlowJo Company	www.flowjo.com
BD FACSDIVA Software	BD Biosciences	www.bdbiosciences.com/us/instruments/research/software/flow-cytometry-acquisition/bd-facsdiva-software/m/111112/overview
Fiji package of Image J	(Schindelin et al., 2012)	fiji.sc
GraphPad Prism v.5	GraphPad Software	www.graphpad.com/scientific-software/prism
Fusion Solo S Western Blot and Chemi Imaging System	Vilber Lourmat	www.vilber.com/fusion-solo-s

CONTACT FOR REAGENT AND RESOURCE SHARING

Further information and requests for resources and reagents should be directed to and will be fulfilled by the Lead Contact, Lenka Besse (lenka.besse@kssg.ch).

EXPERIMENTAL MODEL AND SUBJECT DETAILS

Cell Lines

Cell lines RPMI-8226, AMO-1 and L363 were obtained from commercial sources (American Type Culture Collection, ATCC, Wesel, Germany; Deutsche Sammlung von Mikroorganismen und Zellkulturen, DSMZ, Braunschweig, Germany) and were maintained under standard conditions in RPMI-1640 medium (Sigma-Aldrich, MO, USA) supplemented with 10% heat-inactivated fetal bovine serum (FBS), 100 µg/ml streptomycin and 100 U/ml penicillin (Sigma-Aldrich, MO, USA). Cells were adapted to bortezomib (AMO-BTZ, RPMI-BTZ and L363-BTZ) and carfilzomib (AMO-CFZ, RPMI-CFZ and L363-CFZ) by continuous exposure to increasing drug concentrations as previously described (Soriano et al., 2016). Cell lines were routinely tested for mycoplasma contamination using the MycoAlert™ Mycoplasma Detection Kit (Lonza, Switzerland) and STR-typed to confirm the authenticity of the derived cell line with parental cell lines (Braunschweig, Germany).

Primary Cells

Primary cells were obtained from relapsed, pretreated MM patients during routine diagnostic procedures after approval by the independent cantonal ethical committee and after obtaining written informed consent form. Where necessary, primary cells were enriched by Ficoll density gradient centrifugation. Primary cell preparations were analyzed microscopically after routine staining and only preparations with > 80% malignant cells were used for experiments described here. Patients' baseline characteristic is as follows.

Sample	Age	Sex	Number of Previous Treatment Lines	PCs Site	Previously Refractory to BTZ	Previously Refractory to CFZ	Extramedullary Manifestation	Primary PCL	Secondary PCL
MM1	51	F	3	Peripheral blood	yes	yes	yes	no	yes
MM2	74	F	5	Bone marrow	yes	yes	no	no	no
MM3	61	M	0	Pleural effusion	no	no	yes	no	no

Balb/c Mice

Age-matched (8-10 weeks old) female Balb/c mice were obtained from Charles River, Germany, and kept in isolated ventilated cages with food *ad libitum*. The study was carried out in accordance with the 3Rs principle. Experiments were approved by the Committee for Animal Experiments (St Gallen, Switzerland), application no. 26311.

METHOD DETAILS

Proteasome Subunit Selective Inhibitors

For subunit-selective proteasome inhibition, following concentration of chemicals synthesized at the Leiden Institute of Chemistry, Leiden University, were used:

Selective Inhibitor	Target	Concentration
LU001i	β1i	2µM
NC001	β1c/i	10µM
LU002i	β2i	2µM
LU002c	β2c	6µM
LU025c	β5c	3µM
LU015i	β5i	3µM
LU102	β2c/i	3µM
NC005	β5c/i	5µM

Activity-Based Probes Labelling

Activity of proteasome subunits 1h after treatment with proteasome inhibitors was assessed using the recently developed set of subunit-selective activity based probes (ABP) that differentially visualize individual activities of β1, β2 and β5 subunits of the constitutive and immunoproteasome (de Bruin et al., 2016). Briefly, cellular pellets were lysed with a lysis buffer (1 mM DTT, 5 mM MgCl₂, 10% glycerol, 50 mM Tris-HCl, 2 mM ATP, 0.2% NP-40, 0.5% digitonin, adjusted pH for 7.4) for 10 min/4°C for protein extraction.

Protein content of each sample was measured using Bradford method (Roti-Nanoquant, Carl Roth, Germany) and proteins were adjusted for 30 $\mu\text{g}/9.5 \mu\text{l}$ per sample with dilution buffer (1 mM DTT, 5 mM MgCl_2 , 10% glycerol, 50 mM Tris-HCl, 2 mM ATP) and incubated with 0.5 μl 20x ABP cocktail (final concentration of compounds is: 100 nM Cy5-NC001, 100 nM BODIPY(TMR)-NC005-VS and 30 nM BODIPY(FL)-LU112) for 1h at 37°C. Then, proteins were denatured by 2 min incubation at 95°C, loaded on a gel, separated by SDS-PAGE and visualized by Fusion Solo S Western Blot and Chemi Imaging System (Vilber Lourmat, France).

In Vivo Drug Distribution

Balb/c mice were injected i.v. or i.p. with bortezomib (1 mg/kg) and carfilzomib (4 mg/kg) or with vehicle. Two hours after the drug administration, mice were sacrificed by cervical dislocation and the organs (brain, heart, lungs, spleen, liver, kidneys, bone marrow and PBMC) were isolated.

Bortezomib

Bortezomib was dissolved in DMSO to achieve 2.6 mM stock solution. Out of the stock solution we used 10 μl for 10g of mouse body weight, which was diluted in PBS to achieve 200 μl of final volume per 1 mouse.

Carfilzomib

Carfilzomib was dissolved in DMSO to achieve 5.6 mM stock solution. Out of the stock solution we used 10 μl for 10g of mouse body weight, which was diluted in the vehicle to achieve 200 μl of final volume per 1 mouse.

Vehicle: 10 % Captisol (sulfobutylether- β -cyclodextrin; Cydex pharmaceuticals, Lenexa, Kansas, USA) in 10 mM sodium citrate in PBS (pH 3.5).

Organs and Single Cells Isolation

Mice organs were isolated into cold PBS supplemented with 2mM EDTA. The organs were cut into pieces and passed through the mash/BD cell strainer (40 μm) into 50 ml falcon tubes. Cell suspension was centrifuged at 250g/2min, then suspended in cold Red Blood Cell lysis buffer (BD Biosciences, CA, USA) and incubated for 3 min at RT. This was followed by next round of centrifugation at 250g/2 min until the cell pellet was white, without residual red blood cells. Pellet was washed with cold PBS and then processed for protein extraction and ABP labelling as described above. Bone marrow was isolated into the Eppendorf tubes as described following the protocol (Amend et al., 2016). Next steps from the lysis of red blood cells were the same as described above.

Generation of AMO-1 Ub^{-G76V}-GFP Cells

AMO-1 cells were electroporated with a vector containing Ub^{-G76V}-GFP (obtained from Nico Dantuma; Addgene plasmid #11941) using Gene Pulser Electroporator system (Bio-Rad, CA, USA) and selected using G418 (500ng/ml, Gibco/Invitrogen, MA, USA). The polyclonal culture was subcloned to obtain a single cell derived population using MethoCult (StemCell Technologies, Köln, Germany) and the colony with highest accumulation of fluorescence after PI treatment was chosen for further analyses. Briefly, single-cell derived cell populations were incubated with 100 nM bortezomib for 8h and compared for the intensity of Ub^{-G76V}-GFP by flow cytometry, the population with the highest mean fluorescence intensity was chosen for further experiments.

Flow Cytometry

The functional evaluation of ATP binding cassette ABCB-type activity was performed as described previously (Besse et al., 2018). Briefly, $3 \times 10^5/\text{ml}$ cells were seeded and treated with ABCB-type inhibitor reserpine (10 μM) for 3h, then the cells were incubated with 1 μM MVB003 (an epoxyketone-based pan-reactive probe that was used previously as an ABCB1 substrate) for 30 min/37°C, followed by washing with PBS and analysis by flow cytometer BD Fortessa (BD Biosciences, CA, USA).

For the functional proteasome inhibition, accumulation of GFP fluorescence in AMO-1-Ub^{-G76V}-GFP cells after the treatment was assessed. Cells were treated as indicated for 1h with respective proteasome inhibitors, and GFP fluorescence was acquired after 8h incubation in drug-free media by BD Fortessa flow cytometer (BD Biosciences, CA, USA).

Assessment of Cell Viability

Viability of cells was determined after 48h of treatment by MTS tetrazolium compound using CellTiter 96® Aqueous One Solution (Promega, WI, USA) according to manufactures protocol. For the experiments 1×10^4 cells/well in 96-well plates were seeded.

QUANTIFICATION AND STATISTICAL ANALYSIS

Flow cytometry data were evaluated using FlowJo v10 Software (FlowJo Company, Ashland, OR, USA) and are presented as a mean and \pm SD of median fluorescence intensity (MFI) of at least 3 independent experiments. Gel images were analyzed by Fiji (open source image processing package based on ImageJ) (Schindelin et al., 2012) and are presented as a mean \pm SD of three replicates.

Statistical evaluation was performed in GraphPad Prism v.5 (GraphPad Software, La Jolla, CA, USA). For comparison of three or more groups, one-way ANOVA was used with Tukey post-test, for comparison of two groups unpaired *t*-test was used, values $p < 0.05$ were considered as statistically significant. The coefficient of drug interaction (CDI) was determined as described previously (Li et al., 2016).